On scatterometer ocean stress[1]

M. Portabella, A. Stoffelen

Royal Netherlands Meteorological Institute (KNMI)

Postbus 201, 3730 AE De Bilt, The Netherlands

Phone: +31 30 2206568, Fax: +31 30 2210843

e-mail: portabel@knmi.nl, stoffelen@knmi.nl

[1] Manuscript ref.: Portabella, M., and Stoffelen, A., "On scatterometer ocean stress," submitted to *J. Atm. and Ocean Techn*. in June 2007, © American Meteorological Society.

Abstract

Scatterometers estimate the relative atmosphere-ocean motion at spatially high resolution and provide accurate inertial-scale ocean wind forcing information, which is crucial for many ocean, atmosphere and climate applications. An emprirical scatterometer ocean stress (SOS) product is estimated and validated using available statistical information. A triple collocation dataset of scatterometer, moored buoy and numerical weather prediction (NWP) observations together with two commonly used surface layer (SL) models are used to characterize the SOS. First, a comparison between the two SL models is performed. Although their roughness length and the stability parameterizations differ somewhat, the two models show little differences in terms of stress estimation. A triple collocation exercise is then conducted to assess the true and error variances explained by the observations and the SL models. The results show that the uncertainty in the NWP dataset is generally larger than in the buoy and scatterometer wind/stress datasets, but depending on the spatial scales of interest. The triple collocation analysis also shows that scatterometer winds are as close to real winds as to neutral winds, provided that we use the appropriate scaling. An explanation for this duality is that the small stability effects found in the analysis are masked by the uncertainty in SL models and their inputs. The triple collocation analysis shows that scatterometer winds can be straightforwardly and reliably transformed to wind stress. This opens the door for the development of wind stress swath (level 2) and gridded (level 3) products for the Advanced Scatterometer (ASCAT) onboard MetOp and for further geophysical development.

1 Introduction

Wind forces motion in the ocean and in turn the motion in the ocean determines the weather and climate in large portions of the world. Wind forcing is essential in the El Niño Southern Oscillation (ENSO) and other ocean-atmosphere interaction phenomena, occurring in the Tropics. As such, a homogeneous wind data set of high quality would much advance research on the prediction and mechanisms of seasonal forecasting. *Vialard* (2000) emphasizes that wind stress is certainly the most important forcing in the tropics. Moreover, ocean circulation and ENSO play a key role in the Earth' climate. Besides tropical needs, obvious applications of such wind stress product would be among others in the modelling of the Antarctic circumpolar current, forcing of the southern oceans, research on the variability and occurrence of storms, and forcing in complex basins, e.g., the Mediterranean. A continuous wind stress time series of high temporal and spatial resolution would aid in the understanding of the unexplained variability of these wind events from year to year.

Wind information is available from conventional platform observations, such as ship or buoy. These systems measure the atmospheric flow at a measurement height that can vary between 4 m and 60 m, and are thus not a direct measure of surface 10-m wind nor of stress. Stress computation requires the transformation of these winds by Planetary Boundary Layer (PBL) parameterisation schemes in order to represent the sea surface conditions. These PBL schemes and more in particular, the Surface Layer (SL) schemes embedded in the PBL schemes, have improved accuracy over the years (*Smith et al., 1992*; *Donelan et al., 1993*; *Taylor and Yelland*, 2001; *Bourassa*, 2006) although they still contain transformation errors (*Brown et al., 2005*).

Furthermore, buoy wind observations and, by implication, the NWP analyses that exploit these data use a fixed frame of reference. However, the wind stress depends on the difference of motion between atmosphere and ocean. *Kelly et al.* (2001) show that the ocean currents do produce a significant annual bias in the buoy-derived wind stress estimations. In contrast, they show that scatterometer observations provide a measure of the relative motion between atmosphere and ocean, and therefore can potentially provide accurate wind stress information.

Several authors have pointed to the mesoscale wavenumber gap in NWP wind datasets (e.g., *Chelton et. al., 2004*; *Chelton and Schlax, 1996*; and *Stoffelen, 1996*). This gap is caused by the sparse conventional observations at the sea surface, but also aloft since NWP data assimilation systems are 4-dimensional (4D) in nature and thus require 4D observations to achieve uniform quality. In fact, mesoscale atmospheric waves are poorly observed. Scatterometers, however, do have the capability to observe the surface component of the wind variability on much finer space and time scales. Moreover, scatterometers provide information on the inertial scale of ocean models and thus can potentially provide essential information to drive ocean models (e.g., *Milliff, 2005*; *Chelton et al., 2004*; *Chelton and Schlax, 1996*).

Scatterometer wind and stress retrieval

A scatterometer measures the electromagnetic radiation scattered back from ocean gravity-capillary waves and it is difficult to validate quantitatively the relationship between the roughness elements associated with gravity-capillary waves and the measurements. As such, empirical techniques are employed to relate microwave ocean backscatter with geophysical variables. Since the launch of the Earth Remote Sensing Satellites, ERS-1 (on 17 July, 1991) and ERS-2 (on 21 April, 1995), with on

board the active microwave instrument (*Attema, 1991*) operating at 5.4 GHz (C band) numerous retrieval optimisations and validation studies have been carried out. Usually the retrieved products from satellite scatterometers are validated by collocation with NWP model (e.g., European Centre for Medium Range Forecast, ECMWF) background winds, and/or buoy measurements (*Stoffelen*, *1998a*). A multitude of wind observations is available at a reference height of 10 m, and as such scatterometer winds are traditionally related to 10m winds. For ERS scatterometers, the so-called CMOD-5 (*Hersbach et al., 2007*) Geophysical Model Function (GMF), which relates the 10-meter wind to the backscatter measurements, is used nowadays by the European Space Agency (ESA) and the Royal Netherlands Meteorological Institute (KNMI) for wind retrieval. *Stoffelen* (1998a) shows that for varying ocean wind conditions, the backscatter measurements vary along a well-defined conical surface in the 3D measurement space, i.e., the measurements depend on two geophysical variables or a 2D vector. CMOD-5 indeed well explains the coherent distribution of backscatter measurements in measurement space.

Chelton et al. (2001) and *Stoffelen* (2002) show a high correlation between scatterometer-retrieved winds and kinematic wind stress. In fact, scatterometers respond to sea surface roughness (rather than 10-meter wind), which is closely associated with the wind stress. So, if one collocates wind stress or its equivalent value at 10-meter height (i.e., 10-m neutral wind) to CMOD-5 winds and estimates their relationship, one would obtain a CMOD-5 stress model (or CMOD-5 neutral wind model) that potentially explains more of the backscatter variance than the CMOD5 wind model, since the disturbing effects of atmospheric stratification in the lowest 10m have been eliminated. The GMF would provide the same conical fits in 3D measurement space, since only an argument of the CMOD function has been

transformed. For example, *Milliff and Morzel* (2001) use a 10-m neutral wind GMF to transform SeaWinds scatterometer winds to stress.

The aim of this paper is to define and validate a scatterometer transformation from wind speed^2 to wind stress. For such purpose, triple collocations of ERS-2 scatterometer observations, moored buoy observations and ECMWF model output are performed. Since the tropics and the extra-tropics have very different characteristics in terms of, e.g., wind variability, atmospheric stability or sea state, two different triple collocation datasets, one for each region, are used in this paper (see section 2).

Given the inaccuracy of the SL models (*Smith et al., 1992; Taylor and Yelland, 2001; Bonekamp et al., 2002*), prior to transforming scatterometer wind to stress, we first take a close look at them and compare their performances. For such purpose, two of the most commonly used models, i.e., the LKB model (*Liu et al., 1979*) and the ECMWF SL model (*Beljaars, 1997*), are compared in section 3, where atmospheric stability and wave age effects are analysed in detail for a fixed geophysical data set. The inter-comparison reveals some small and interesting differences in the SL models.

Stoffelen (1998b) shows that given a triple collocation dataset, the uncertainty of the three observing systems can be uniquely determined, provided that one of the systems is used as reference for calibration (scaling) of the other two systems. In section 4, we perform the triple collocation exercise as described by *Stoffelen* (1998b) to assess the random error and scaling properties of both buoy and NWP wind stress derived from the SL models and evaluate the common true variance and system error variances for winds at different heights. As such, the triple collocation exercise is used to

characterise the scatterometer ability to measure kinematic wind stress rather than wind, and to recommend a wind-to-stress transformation for the ERS scatterometer. Finally, a summary of the work and recommendations for future developments are presented in section 5.

2 Data

Two triple collocation datasets for the years 2000 (tropical data) and 1999/2000 (extra-tropical data) are generated to carry out the work described in this paper. The three data sources used in these datasets are the ERS-2 scatterometer, the moored buoy network, and the ECMWF model.

KNMI produces the scatterometer wind and stress products within the Ocean & Sea Ice (OSI) and Climate Monitoring (CM) Satellite Application Facilities (SAFs) of the European Organisation for the Exploitation of Meteorological Satellites (EUMETSAT), and develops scatterometer wind processing software in the Numerical Weather Prediction (NWP) SAF. In the framework of these SAFs, KNMI has developed an ERS scatterometer data processing (ESDP) package for the generation of operational wind products. As such, ERS-2 ESDP (version 1.0g) 10-m winds are used in this study.

The tropical moored buoy data used correspond to the National Oceanic Atmospheric Administration (NOAA) TAO and PIRATA buoy arrays, which are located in the tropical Pacific and Atlantic oceans, respectively (see Figure 1). The quality-controlled data are available online at the following NOAA sites: http://www.pmel.noaa.gov/tao and http://www.pmel.noaa.gov/pirata.

[2] Note that the transformation only refers to wind and stress intensities since the direction of the air flow is assumed to be constant in the SL.

Due to the limited number of extra-tropical moored buoys available online, buoy data distributed through the Global Telecommunication System (GTS) stream, quality controlled and archived at ECMWF, and kindly provided by Jean-Raymond Bidlot are used instead. Open ocean buoy data from the National Data Buoy Centre (NDBC), the Marine Environmental Data Service (MEDS), and the UK Met Office, which are located in the extra-tropical North Pacific and North Atlantic oceans, are used (see Figure 1). Details on the data quality control (QC) can be found in *Bidlot et al.* (2002). Note that, because of how the GTS data are encoded, the individual wind observations are only available to the closest m/s.

Hourly sea surface winds together with other surface layer relevant parameters, such as sea surface temperature (*SST*) and air temperature (*T*) are retrieved from the buoy data files. Additionally, first guess (FG) ECMWF ERA-40 lowest level (approximately 10 meter height) winds, *T,* specific humidity (*q*), pressure (*p*), *SST*, surface pressure (*sp*) and Charnock parameters are retrieved from the ECMWF MARS archive. FG winds do not contain the observed information in the scatterometer and buoys used in the triple collocation, such that the FG error and the observed wind errors may be assumed independent.

The triple collocations are performed in the following way. The ESDP collocation software is used to spatially and temporally interpolate (linear in space and cubic in time) the 3-hourly and 1.1° ECMWF ERA-40 forecast data to the ERS-2 scatterometer data acquisition location and time, respectively. In our experience, interpolation errors are negligible using this scheme. Then the ECMWF-ERS dataset is collocated to the moored buoy dataset using the following criteria: only observations separated less than 25 km in distance and 30 minutes in time are

included in the ECMWF-ERS-BUOY triple collocation dataset. This implies only one ECMWF-ERS observation (the closest) per buoy observation. In practice, most of the collocations are within 12.5 km and 10 minutes, thus considerably reducing the collocation error, i.e., uncertainty due to spatial and temporal separation between collocated observations.

Several Quality Control (QC) procedures have been applied to this dataset. The nominal ESDP QC procedure (*Stoffelen, 1998a*) is applied to the ERS-2 retrieved wind dataset and only the buoy data with the "highest quality" flag are used. Moreover, a 4-sigma test is performed to the triple collocated dataset as in *Stoffelen* (1998b). The tests are carefully designed in order to maintain the main shape of the wind probability density functions (PDFs).

To avoid uncertainties from unnecessary SL model height transformations, it seems appropriate to use wind datasets from a fixed height. In this respect, the ECMWF ERA-40 winds used in here correspond to the lowest model level, i.e., about 10 meter height. Since the extra-tropical buoy dataset contains many different buoy systems with different observation heights, a compromise between the number of buoys and the observation height spread is needed. In this paper, only buoy stations with anemometer heights between 4 and 5 meters are considered (note that all tropical buoys have a fixed anemometer height of 4m). In total, we use data from 53 tropical buoy stations and 41 extra-tropical buoy stations, which produced 3471 and 3345 collocations (after quality control), respectively, over the mentioned periods.

3 Surface layer model comparison

Most of the equations that describe the physical balances and the turbulent budgets in the lowest 10% of the PBL, i.e., the surface layer, cannot readily be solved, due either to the presence of highly nonlinear terms or the requirement for enormous in-situ data bases (*Geernaert, 1999*). One can alternatively characterize the flow's dominant dynamic, geometric, and temporal scales, which involve characteristic time, space, or velocity scales, by dimensionless groups of variables. The similarity theory, first postulated by *Monin and Obukov* (1954), states that there exists such groups of variables which have functional relationships to the flow field and/or fluxes, and these in turn can be used to characterize the behavior of the higher order terms of the above mentioned equations.

The surface layer is assumed to be a constant flux layer and it extends up to a few tens of meters above the surface. In the bulk parameterization of the similarity theory, the fluxes are determined with the transfer coefficients which relate the fluxes to the variables measured, e.g., surface wind speed (U), T, SST, q. The bulk transfer coefficients can be determined by integrating the U, T and q profiles. Close to the surface, the distributions of U, T and q are governed by diabatic processes. As such, the wind profile can be written as (e.g., *Businger 1973*):

$$u_* = \frac{k}{[\ln(\frac{z}{z_0}) - \psi(z/L)]}(U - U_s) \qquad (1)$$

where k is the von Karman constant, u_* is the friction velocity, z is the height above the surface, z_0 is the roughness length for momentum, ψ is the stability function for momentum (positive, negative, and null, for unstable, stable, and neutral conditions,

respectively) and L is the Monin-Obukhov length, which includes the effects of temperature and moisture fluctuations on buoyancy. The wind at the surface U_s is neglected (current effects are statistically investigated in section 4.4). Similar profiles to the one in Eq. 1 are also derived for the scale temperature (T_*) and the scale humidity (q_*) (see *Liu et al., 1979*). Since stability (z/L) depends on T and q, the set of 3 dimensionless profiles (u_*, T_*, and q_*) have to be solved at the same time.

Although the paper seeks for the transformation of wind to kinematic wind stress (u_*^2) for scatterometers, in order to provide a scatterometer wind stress (τ) end product (SOS), knowledge of the air density (ρ) is required, i.e., $\tau = \rho \cdot u_*^2$. Air density variations can be large. However, ρ error, which depends on surface pressure, air temperature, and humidity, is generally small (1-2%) and can exceptionally increase locally in cases such as cold air outflow.

In order to solve for u_*, the wind at certain height, among other parameters, is required and z_0 and L must be estimated (see Eq. 1). Once u_* is estimated, the SL models can be used to compute the wind at any height (within the SL) and any stability, e.g. neutral wind, just by modifying z and L, respectively, in Eq. 1. In other words, given a wind observation at certain height (within the SL), we can estimate the winds at any other height and stability, provided that we first estimate kinematic stress.

The discussion of air-sea transfer is not about the validity of the approach described above but generally about the details of parameter and function choices. As such, most SL models are based on the bulk formulation derivation (e.g., Eq. 1), and differences among them lie in the parameterization of L and/or z_0. This is the case for

the two SL models used in this work, i.e., the LKB and the ECMWF SL models. Their similarities and differences are further discussed in the following section.

3.1 LKB versus ECMWF: formulation

The LKB and ECMWF SL models present the same roughness length function (see *Liu and Tang, 1996*, and *Beljaars, 1997*), which is written as:

$$z_0 = \frac{0.11 \cdot \nu}{u_*} + \frac{\alpha \cdot u_*^2}{g} \tag{2}$$

where ν is the kinematic viscosity of the air (1.5×10^{-5} m^2/s), g is the gravitational constant of the Earth (9.8 m/s^2), and α is the (dimensionless) Charnock parameter (see *Charnock, 1955*). However, the Charnock value, which is a sea-state parameter, is substantially different, i.e., 0.011 for LKB and around 0.018 for ECMWF SL (the latter is not a fixed value).

The same happens with the formulation of the stability function $\psi(z/L)$, which is identical for both models, but where the computation of the L parameter (Monin-Obukhov length) differs from one another (see *Liu et al., 1979*, and *Beljaars, 1997*).

The stand-alone ECMWF SL model uses as input U, T, q, pressure (p), observation height (z), *SST*, surface pressure (*sp*), and Charnock data. Similar input is used in LKB; the main difference is that no Charnock input but a default value of 0.011 is used instead. If q information is not available, LKB also allows relative humidity (*rh*) observations as input. Both SL models can solve for wind stress provided that U, T, and *SST* are available. That is, when humidity and pressure observations are not available, default values are used instead. Those values are slightly different, i.e., *rh*=0.8 and *sp*=1013 hpa for LKB versus *rh*=1 and *sp*=1000 hpa for ECMWF.

Additional differences between the two models are reported in detail in *Stoffelen et al.* (2006) and *Portabella and Stoffelen* (2007) and are found to be minor.

3.2 LKB versus ECMWF: results

In this section, we present the most relevant results of comparing the LKB model against the ECMWF SL model, using the tropical and extra-tropical datasets described in section 2. A more detailed comparison of the two SL models can be found in *Stoffelen et al.* (2006) and *Portabella and Stoffelen* (2007).

Figure 2 shows the two-dimensional histogram of LKB estimated u_* versus ECMWF SL estimated u_* for two different extra-tropical input datasets: GTS buoys (left plot) and ECMWF model output (right plot). Since the two datasets contain different parameters (see discussion in section 2) and the two SL models allow somewhat different input (see section 3.1), we use the coincident parameters (U, T, and SST) for all 4 combinations. As it is clearly discernible, the distribution lies close to the diagonal, it is very narrow, and the correlation is 1, meaning that the estimated u_* is very similar, regardless of the SL model or the dataset used. Very similar results are found when using the tropical datasets as input (not shown). In other words, the two models show very similar stresses.

A 5% bias at high u_* values needs to be explained, though. As described above, SL model differences must lie in the roughness length and the stability parameters. Therefore, we take a closer look at these.

3.2.1 Roughness term

Figure 3 shows the same as Figure 2b, but for the z_0 parameter. Again, the correlation between the two models is striking. However, a clear difference between the two model formulations is noted. As discussed in section 3.1, the Charnock parameter is substantially different for both models, i.e., 0.011 for LKB and 0.018 (default value) for ECMWF. Therefore, for very low u_* values, where the viscosity term (first right-hand side term of Eq. 2) is dominant, the distribution lies on the diagonal (same z_0 for both models), and for higher u_*, where the Charnock term is dominant (second right-hand side term of Eq. 2), the distribution is off diagonal, with a slope which is given by the ratio between the Charnock values of both models.

Looking at Figures 2b and 3, one can easily realize that in order to achieve such good agreement in u_* (Figure 2), the stability term in Eq. 2 has to compensate for the difference in the roughness term between the two models. Given the fact that the roughness term is logarithmic, the difference between LKB roughness term and ECMWF roughness term is just a constant, i.e., $\ln\left(\frac{z}{z_0^{ECMWF}}\right) = \ln\left(\frac{z}{z_0^{LKB}}\right) - c$, where $c = \ln(\frac{\alpha^{ECMWF}}{\alpha^{LKB}}) \cong 0.5$ (using the already mentioned LKB and ECMWF default Charnock values). Since the roughness term $\ln\left(\frac{z}{z_0^{LKB}}\right)$ values vary between 13 (low z_0) and 9 (high z_0), provided that the stability term is relatively small in both models, there should be a scaling of about 5% between ECMWF and LKB u_*, which is not present at low u_* values (see Figure 2).

3.2.2 Stability term

The relative weight of the stability term in the denominator of Eq. 1 is analysed for both the LKB and the ECMWF SL models. It turns out that the stability term is only relevant for low z_0 values (i.e., low winds) (not shown). This is consistent with the bias observed in Figure 2, i.e., the constant c becomes relevant at increasing z_0, since the stability impact becomes marginal and $\ln\left(\frac{z}{z_0^{LKB}}\right)$ decreases. Moreover, the LKB stability term is more relevant than the ECMWF stability term. Since most of the observations correspond to unstable ($\psi > 0$) situations (see Figure 4), the more relevant stability term for LKB compensates the larger z_0 values from ECMWF SL model, such that the resulting u_* values are very similar for both models.

Given the fact that both SL models use the same stability functions (ψ), we can easily prove that LKB estimates larger instability (higher negative z/L values) than ECMWF. Figure 4 shows the histogram of the stability parameter (z/L) for both the LKB model (solid line) and the ECMWF SL model (dotted line), using the extra-tropical ECMWF dataset as input. We note larger accumulations at large negative z/L values for LKB than for ECMWF SL, indicating larger estimated instability in the former model. Also note that the stability term is small for stable cases since these are close to neutral stability (i.e., no cases with large positive z/L). Similar results are found in the tropics (not shown).

3.2.3 Sea state effects

The Charnock parameter is a measure of wave growth, hence wave age. As mentioned in section 3.1, the Charnock parameter is fixed for LKB but not for ECMWF SL

model. The Charnock parameter, as formulated in the ECMWF Wave model (WAM) (see documentation at http://www.ecmwf.int/research/ifsdocs/CY28r1/Waves/), is a function of the so-called wave induced stress which in turn is function of the wind input source term (*Janssen, 2004*). Such Charnock output is included in the collocated ECMWF dataset (see section 2) and therefore can be used as input to the ECMWF SL model.

Up to now, results have been produced with fixed Charnock values (default values) for both models, i.e. 0.011 for LKB and 0.018 for ECMWF. To show the impact of a variable Charnock (i.e., sea state dependency) on the estimated u_* uncertainty, we focus the analysis in the region where the sea state is most relevant, i.e., the extra-tropics (see *Portabella and Stoffelen, 2007*). As such, Figure 2b is reproduced with (variable) ECMWF Charnock input. The 2-D histogram in Figure 5 shows only larger spread than the one in Figure 2b, as indicated by the different Standard Deviation (SD) scores. However, as indicated by the correlation score in Figure 5 (very close to 1), the spread is relatively small. Even if the sea state is more relevant in the extra-tropics than in the tropics, it has little impact on the wind stress (u_*) estimation.

The triple collocated dataset can be used to better analyze the Charnock output from WAM. Figure 6 shows the scatterometer – ECMWF (left plot) and buoy – ECMWF (right plot) speed bias and SD as a function of the Charnock parameter in the extra-tropics. ECMWF and GTS buoy speeds have been converted to 4 m height speeds using ECMWF SL model. Since the scatterometer actually observes sea surface roughness, which is directly affected by the wave induced stress, one would expect that for increasing Charnock (sea state) values, sea surface roughness and therefore the mean biases in the left plot would increase. However, the bias is rather flat and

very similar to the one in the right plot, where for the same set of points no explicit roughness effect is expected. Moreover, the spread in the data points could be different due to sea state effects, which is also not the case and the plots look very similar indeed. The wind vector cell, WVC, mean sea state roughness as observed by scatterometers thus appears mainly wind-driven and cases of substantial stress-wind decoupling appear exceptional. The slight bias increase at large Charnock values in the left plot may be an indication of stress-wind decoupling, although there is not enough data to support this statement. It is therefore concluded that, in general, Charnock is very much correlated to the WVC-mean wind and therefore has small impact in the quality of a global SOS[3]. However, the Charnock parameter may contain some added value for exceptional conditions such as cases of extreme wind variability and/or air-sea temperature difference. A much larger dataset is needed however to further investigate this.

3.2.4 Atmospheric stability effects

The impact of stability on wind stress estimates is often measured by the difference between the actual wind (U) and its equivalent neutral wind (U_n), i.e., the wind that results from estimating u_*, given a wind observation at certain height z and under certain atmospheric stability (z/L), and subsequently using such u_* to solve Eq. 2 at the same height z assuming neutral stability (i.e., ψ=0).

Figure 7 shows the difference between U_n and U as a function of U using the LKB model, for the tropical (left plot) and extra-tropical (right plot) buoy input datasets. In the tropics (Figure 7a), differences between neutral winds and actual wind tend to

[3] Note that same conclusions are drawn when repeating the same exercise using calibrated (see section 4) scatterometer winds.

increase for low winds (below 3 m/s) and then slightly decrease for increasing speeds. In the extra-tropics (Figure 7b), this pattern is less evident, due to the presence of a wider range of stratification (stronger stable and unstable situations), although still present. The same pattern is produced when using ECMWF SL model instead of LKB and/or ECMWF input instead of buoy input (not shown). It is clear from Figure 7 that stability effects are small both in the tropics and the extra-tropics and generally within the range [0, 0.3] m/s.

4 Wind-to-stress characterization

In remote sensing, validation or calibration activities can only be done properly when the full error characteristics of the data are known. In practice, the problem is that prior knowledge on the full error characteristics is seldom available. *Stoffelen* (1998b) shows that simultaneous error modeling and calibration can be achieved by using triple collocations. Simultaneous error modeling and calibration can be used to compare triple collocation wind component datasets. In this section, the scatterometer winds are fixed in all datasets and used as reference. The two other wind observing systems (i.e., buoys and NWP) are presented at varying heights and stability conditions, such that the true and error variances can be evaluated for the different datasets. In this way, the interpretation of the different observing systems and the performance of the SL models are characterized in this section.

4.1 Triple collocation exercise

Stoffelen (1998b) shows that when the three observing systems represent the same spatial scales, the triple collocation procedure can resolve the uncertainty of the three systems, provided that one of them is used as reference for calibration. When the

systems do not represent the same resolution, we have to take into account the spatial representativeness error[4]. In particular, we need to make an assumption on the correlation of the spatial representativeness error, i.e., the (true) variance common to the two systems that can resolve the smaller scales[5].

In our case, we have one system, i.e., ECMWF, which resolves large scales (typically > 200 km) and two systems, which can resolve smaller scales, i.e., buoy and scatterometer. Since the scatterometer resolves wind component scales of about 50 km, the true wind component variance on spatial scales of 50 to 200 km is resolved by both scatterometer and buoys, but not by ECMWF (*Stoffelen, 1998b*). For three similar observing systems to the ones used in this work, i.e., the National Oceanic and Atmospheric Administration (NOAA) buoy winds, ERS scatterometer winds, and National Centers for Environmental Prediction (NCEP) model winds, *Stoffelen* (1998b) estimated a correlated representativeness wind component error (r^2) of 0.75 m^2/s^2 in the extra-tropics. We assume the same r^2 value for the 50-to-200 km scale true wind component variance here. In the tropics, and because of the generally lower small-scale wind variability (trade winds) with respect to the extra-tropics, we assume an r^2 of 0.25 m^2/s^2.

4.2 Error assessment using LKB and ECMWF SL models

The triple collocation exercise is used here to assess the random errors and scaling properties of the ERS scatterometer, buoy and ECMWF winds, using ERS scatterometer CMOD-5 winds as a reference system. As such, the performance of the

[4] When comparing two observing systems with different spatio-temporal resolution, the variability of the higher resolution system at the scales that are not resolved by the lower resolution system may be interpreted as error, i.e., a spatial representativeness error. In fact, this variability is resolved true variance of the higher resolution system.

two SL models compared in section 3, i.e., LKB and ECMWF, can be tested by using the SL models to convert buoy and ECMWF wind observations to different reference heights (e.g., 4 m, 10 m) and then estimating the errors of the buoy and NWP converted wind "observations".

Table 1 shows the true variability and the observation error for tropical and extra-tropical datasets, when LKB is used to produce the (buoy and NWP) wind datasets at 10-m height. Note that the scores are given in terms of wind vector SD (computed from wind component SD) rather than wind vector variance (square of SD value) since the former is most commonly used to refer to wind variability and observation errors. The true variability in the extra-tropics (7.48 m/s) is comparable to the one estimated by *Stoffelen* (1998b) (7.03 m/s) and substantially larger than the tropical values (5.79 m/s). This is an expected result since the wind variability is known to be substantially lower in the tropics than in the extra-tropics.

The correlated part of the representativeness error, as mentioned above, represents the common variance in the higher resolution systems, i.e., the scatterometer and the buoys. Therefore, when performing data interpretation for high resolution applications, e.g., development of 25-km or 50-km wind products, this common variance is considered as part of the true variance, but as part of the error (lack of high-resolution information) of the lower resolution system, i.e., NWP model. Table 2 accounts for such interpretation. On the other hand, when looking at lower resolution applications, e.g., NWP data assimilation, this common variance cannot be resolved and is therefore interpreted as part of the (spatial representativeness) error of the higher resolution systems, i.e., scatterometer and buoy. Note that Table 1 shows the

[5] This common variance is, in fact, the resolved true variance embedded in the representativeness error of both systems.

same as Table 2 but accounting for the latter interpretation. We also note that differences between the two tables are produced by the assumed r^2 value, which is small compared to true variance and generally modest compared to the error variances.

When ECMWF SL model is used (instead of LKB) to produce the (buoy and NWP) wind datasets at 10-m height, the triple collocation results (not shown) are almost identical to the ones in Tables 1 and 2. That is, the performance of both SL models is comparable. These results are in line with the results of section 3, where both models were showing little differences. The same exercise is repeated using buoy and NWP winds at 4 m height, i.e., the approximate measurement height of buoys. In this case, no SL model transformation is required for the buoy winds. The results (not shown) are very similar in terms of true variability and errors of the different sources, denoting that the SL model does not introduce additional error when buoy winds are transformed from 4m to 10m. It also implies that scatterometer winds can be scaled equally well to 10m and 4m winds.

However, when performing triple collocation, the scaling factor for buoy (i.e., the buoy-to-scatterometer wind calibration value) is closer to one at a reference height of 4 m than at 10 m, meaning that CMOD5 scatterometer winds should be interpreted as 4-m winds rather than 10-m winds.

4.3 Scatterometer wind interpretation

As discussed in the introduction, scatterometers are essentially observing wind stress. Therefore, one may better interpret scatterometer-derived winds as equivalent neutral winds (i.e., stress) rather than real winds. In this section, we investigate the

interpretation of scatterometer data by performing the triple collocation exercise for two different datasets:

- ERS CMOD-5 winds, buoy real winds, and ECMWF real winds;
- ERS CMOD-5 winds, buoy neutral winds, and ECMWF neutral winds.

The first dataset is the same as the one used in section 4.2. The second dataset is the same as the first one but for buoy and NWP converted neutral winds using either LKB or ECMWF SL model. As in section 4.2, ERS scatterometer CMOD-5 winds are used as reference.

The true variability and error scores of dataset a) (see Tables 1 and 2) are very similar to the scores obtained with dataset b) (see Tables 3 and 4), when using LKB model and 10-m conversion. The same conclusions are drawn when using ECMWF SL model and/or 4-m conversion. This indicates that scatterometer winds can explain the same true variability regardless of whether these are tested against real or neutral winds. That is, scatterometer winds are as representative of real winds as they are of equivalent neutral winds (or stress).

In order to reinforce such conclusion, and given the fact that CMOD-5 GMF was tuned to 10-m real (NWP) winds, we develop a new GMF (CMOD-5n) by tuning our CMOD-5 real winds to neutral winds. Figure 8 shows the bias of CMOD-5 winds with respect to 10-m buoy real winds (solid) and 10-m buoy neutral winds (dotted) as a function of wind speed[6]. By subtracting these two curves, i.e., about 0.2 m/s in the tropics (Figure 8a) and 0.1 m/s in the extra-tropics (Figure 8b), we derive a statistical

[6] Since most of the times there is unstable stratification (see Figure 4), the real winds are biased low with respect to the equivalent neutral winds at any reference height within the SL.

real-to-neutral conversion (dashed) that can be used to derive CMOD-5n from CMOD-5.

We then perform the same triple collocation exercise as before but using ERS CMOD-5n winds instead of CMOD-5 winds in datasets a) and b) as a reference. As expected, the results are again very similar.

The fact that scatterometer winds are statistically as close to real winds as to neutral winds can be explained as follows: on the one hand, the stability effects are small, i.e., differences between real and neutral winds are subtle (see Figure 7 in section 3.2); on the other hand, SL models and the different observations (wind, SST, air temperature) used by the models to compute height conversions and neutral winds contain errors, which in turn mask the already subtle differences between real and neutral winds (*Stoffelen et al., 2006; Portabella and Stoffelen, 2007*).

Although scatterometer winds can be interpreted as real winds from a statistical point of view, there may be special air-sea interaction situations where the scatterometer shows its real potential to measure stress. For example, note that a difference of 0.2 m/s exists between neutral and real winds using the tropical data set. The extra-tropical difference (i.e., 0.1 m/s) is smaller mainly because of cases with stable stratification that appear below the main cloud of points in Figure 7. For these single cases, the use of stability information may increase the true variability in a triple collocation exercise, therefore indicating that such scatterometer observations should be interpreted as neutral winds (or stress) rather than real winds. To prove this, further tests with a larger dataset are required.

4.4 Scatterometer wind-to-stress transformation

In order to obtain stress, first a well-calibrated scatterometer 10-m neutral wind is required. Then a SL model like LKB or ECMWF SL can be used to convert 10-m neutral winds to wind stress. In fact, since the most recently developed SL models (*Taylor and Yelland, 2001*; *Bourassa, 2006*) have similar performance up to 16 m/s (*Bourassa, 2006*), either one of them can be used to do the neutral-to-stress conversion. Since no stability information is needed to do this conversion, an independent scatterometer ocean stress (SOS) product can be developed straightforwardly.

To obtain the calibrated scatterometer 10-m neutral wind, a scatterometer-to-buoy correction (calibration) and a real-to-neutral wind conversion need to be applied to CMOD-5 winds. The combined correction and conversion is represented by the dotted curves in Figure 8, which have a different mean (absolute) value of 0.8 m/s in the tropics (Figure 8a) and 0.55 m/s in the extra-tropics (Figure 8b). The latter further confirms the results from *Hersbach et al.* (2007) with a similar extra-tropical dataset.

Several effects may lead to these differences between tropical and extra-tropical datasets. The most relevant are, on the one hand, the large wind variability in the extra-tropics, and, on the other hand, the effect of currents in the tropics. In order to recommend a final combined correction value, an analysis of the uncertainties of the triple collocation exercise (mainly produced by the mentioned effects) is performed. One way to analyze such uncertainties is to take the calibrated dataset (after triple collocation) and examine the residual biases buoy by buoy. As such, we compute the residual wind component (the west-to-east U and the south-to-north V wind components) buoy and ECMWF biases against scatterometer at each buoy location.

Table 5 shows the average and SD of the mentioned wind component residual biases. Only buoy locations with at least 50 triple collocations, i.e., 34 tropical and 30 extra-tropical buoy locations, are used in the statistics. The uncertainty found in the extra-tropics (SD of about 0.2 m/s) is consistent with the expected wind variability effect. A comparable result is found for the tropical dataset, indicating that the uncertainties produced by, e.g., the currents in the tropics, are comparable to the ones produced by, e.g., the large wind variability in the extra-tropics. In other words, for a global correction both combined correction values (i.e., 0.8 m/s found in the tropics and 0.55 m/s in the extra-tropics) have a similar degree of confidence.

Therefore, we recommend adding 0.7 m/s (compromise between the tropical and the extra-tropical values) to CMOD-5 winds to obtain the scatterometer 10-m neutral winds. To obtain real winds we recommend adding 0.5 m/s to CMOD5.

5 Conclusions

Scatterometer backscatter is closely related to ocean kinematic stress. For practical reasons, however, C-band backscatter has been related to real 10-m winds. Effects of stability, currents, and waves could then potentially cause error in the scatterometer interpretation. In this paper, we statistically investigate a physically more direct interpretation of scatterometer backscatter data as kinematic stress or its equivalent 10-m neutral winds.

Since direct stress or roughness measurements are generally lacking for such purpose, a tropical and an extra-tropical triple collocated wind dataset are used, i.e., ERS-2 scatterometer winds, moored buoy data, and ECMWF model output. As a consequence, all comparisons are based on a fixed set of data points and uncertainties

due to a difference in the number or location (e.g., by screening) of the inputs are absent. That is, the geophysical conditions for the comparisons are set fixed and a careful geophysical analysis follows.

First, a comparison between two commonly used SL models, i.e., LKB and ECMWF, is performed. The main difference between the two models is in the roughness length (z_0) and the stability (L) parameterizations. On the one hand, whereas LKB uses a constant Charnock value, ECMWF uses a substantially larger Charnock value. Since the ECMWF roughness parameterization is sea state dependent, its Charnock parameter is moreover variable, in particular in the extra-tropics. On the other hand, LKB has larger instability (larger negative z/L values) with respect to ECMWF. This difference actually compensates for the difference in the roughness formulation for moderate winds, such that the resulting stress values are very similar for both models. At high winds though, the stability term is much smaller than the roughness term and therefore the different roughness formulation results in some small stress bias (about 5%) between the two models.

Another relevant result of this comparison is that sea-state dependent (variable Charnock) effects are small and that the atmospheric stability effects are also small and of the order of ocean current effects. Otherwise, the results show similar performance of both SL models.

To characterize the ability of scatterometers to measure stress and wind, two triple collocation exercises are performed: the first one uses scatterometer CMOD-5 winds together with buoy and NWP real winds; and the second one uses the same data but buoy and NWP neutral winds instead, where neutral winds are a measure of the SL stress. True variability and error scores are almost identical in both exercises, meaning

that scatterometer winds are as close to real winds as to neutral winds, provided that we use the appropriate scaling. A test with scatterometer neutral winds further corroborates such interpretation. An explanation for the duality in scatterometer data interpretation is that the small stability effects are masked by the uncertainty in SL models and their inputs.

The results presented in this paper confirm the ones obtained by *Hersbach et al.* (2007) with a similar extra-tropical dataset. As such, we confirm that an independent ERS scatterometer stress (SOS) product can be obtained by adding 0.7 m/s to CMOD-5 winds and use such result as the 10-m neutral wind input to a recently developed SL model, which is needed to compute stress. [Note that KNMI uses the LKB SL model since it is widely used and publicly available.]. A schematic illustration of the wind-to-stress conversion is shown in Figure 9.

The formulation of the roughness length (Eq. 3) presented by these two SL models is not the only one available. Differences between different formulations have been thoroughly studied. For example, *Bonekamp et al* (2002) claim that a wave age dependent Charnock SL model (such as ECMWF) is marginally better than a constant Charnock model (such as LKB). Moreover, several authors have proposed different wave age dependent parameterizations, e.g., *Donelan* (1990), *Maat et al.* (1991), *Smith et al.* (1992), *Johnson et al.* (1998), and *Drennan et al.* (2003). On the other hand, *Taylor and Yelland* (2001) proposed an alternative wave steepness parameterization of z_0. The work presented in section 4 could be used to compare the performance of additional SL models in interpreting scatterometer measurements.

However, in general, SL model differences in terms of wind stress magnitude are small for winds below 10 m/s, and it is only well above 10 m/s that the different

roughness formulations produce large differences in the estimated stress (see also *Taylor et al., 2001*). Moreover, according to *Bourassa* (2006), the most recently developed SL models (e.g., *Taylor and Yelland, 2001*; *Bourassa, 2006*) have similar performance up to 16 m/s, which is consistent with the comparison of LKB and ECMWF SL models performed in here. However, cases of extreme wind variability or air-sea temperature difference may show large wind and stress discrepancies. The triple collocated datasets used in this paper are not sufficient to properly investigate the performance of the SL models in such extreme cases, where the differences between models may be more significant. As such, a study over a much larger dataset is recommended for such purposes. Moreover, it would also be interesting to study the ability of scatterometers to measure stress in such extreme conditions.

Although the results in this paper relate to the ERS scatterometer, the wind to stress conversion also applies to other scatterometers. A new C-band scatterometer, i.e., ASCAT (onboard MetOp), which has more than twice the coverage of the ERS scatterometer, was launched on October 19, 2006. In the framework of a collaboration between NOAA and EUMETSAT, ASCAT underflights have been planned during the NOAA 2007 winter storm and tropical cyclone campaigns. These extreme weather datasets could therefore be used for the above mentioned purposes.

Acknowledgements

Special thanks go to Jean-Raymond Bidlot and ECMWF for providing the GTS buoy dataset (already quality controlled) together with feedback on the collocation exercise and our results. We acknowledge the help and collaboration of our colleagues working at KNMI, and more in particular the people from the scatterometer group. This work is funded by the European Organisation for the Exploitation of

Meteorological Satellites (EUMETSAT) Climate Monitoring (CM) and Ocean & Sea Ice (OSI) Satellite Application Facilities (SAFs), lead by the Deutscher Wetterdienst (DWD) and Météo France, respectively. The software used in this work has been developed at KNMI, through the EUMETSAT OSI and Numerical Weather Prediction (NWP) SAFs, and at ECMWF.

References

Attema, E. P. W., 1991: The active microwave instrument on board the ERS-1 satellite. *Proc. IEEE*, vol. 79, 791-799.

Beljaars, A. C. M., 1997: Air-sea interaction in the ECMWF model. *Proc. of seminar on atmosphere-surface interaction*, European Centre for Medium-Range Weather Forecasts, Reading, United Kingdom,.

Bidlot J.-R., D. J. Holmes, P. A. Wittmann, R. Lalbeharry, and H. S. Chen, 2002: Intercomparison of the performance of operational ocean wave forecasting systems with buoy data. *Wea. Forecasting*, vol. 17, 287-310.

Bonekamp, H., G. J. Komen, A. Sterl, P. A. E. M. Janssen, P. K. Taylor, and M. J. Yelland, 2002: Statistical comparisons of observed and ECMWF modelled open ocean surface drag. *J. Phys. Oceanogr.*, vol. 32, 1010-1027.

Bourassa, M. A., 2006: Satellite-based observations of surface turbulent stress during severe weather. *Atmosphere-Ocean Interactions*, vol. 2, W. Perrie, ed., Wessex Institute of Technology, 35-52.

Brown, A. R., A. C. M. Beljaars, H. Hersbach, A. Hollingsworth, M. Miller, and D. Vasiljevic, 2005: Wind turning across the marine atmospheric boundary layer. *Quart. J. R. Met. Soc.,* **131** (607), doi:10.1256/qj.03.203, 1233-1250.

Businger, J. A., 1973: Turbulent transfer in the atmospheric surface layer. *Workshop on Micrometeorology*, Amer. Meteorol. Soc., 67-100.

Charnock, H., 1955: Wind stress on a water surface. *Quart. J. R. Meteorol. Soc.*, vol. 81, 639-640.

Chelton D. B., and M. G. Schlax, 1996: Global observations of oceanic Rossby waves. *Science*, vol. 272, 234-238.

Chelton, D. B., S. K. Esbensen, M. G. Schlax, N. Thum, M. H. Freilich, F. J. Wentz, C. L. Gentemann, M. J. McPhaden, and P. S. Schopf, 2001. Observations of coupling between surface wind stress and sea surface temperature in the eastern Tropical Pacific. *J. Climate*, vol. 14, 1479-1498.

Chelton, D. B., M. G. Schlax, M. H. Freilich, and R. F. Millif, 2004. Satellite measurements reveal persistent small-scale features in ocean winds. *Science*, vol. 303, 978-983.

Donelan, M. A., 1990: Air-sea interaction. *The Sea*: *Ocean Engineering Science*, vol. 9, part A, B. LeMéhauté and D. M. Hanes, ed., John Wiley, 239-292.

Donelan, M. A., F. W. Dobson, S. D. Smith, and R. J. Anderson, 1993: On the dependence of sea surface roughness on wave development. *J. Phys. Oceanogr.*, vol. 23, 2143-2149.

Drennan, W. M., H. C. Graber, D. Hauser, and C. Quentin, 2003: On the wave age dependence of wind stress over pure wind seas. *J. Geophys. Res.*, vol. 108(C3), 8062, doi:10.1029/2000JC000715.

Geernaert, G. L., 1999: Theory of air-sea momentum, heat and gas fluxes. *Air-sea exchange: physics, chemistry, and dynamics*, G. L. Geernaert, ed., Kluwer Academy Publishers, Boston, 25-48.

Hersbach, H., A. Stoffelen, and S. de Haan, 2007: The improved C-band ocean geophysical model function CMOD-5. *J. Geophys. Res.*, vol. 112 (C3), doi:10.1029/2006JC003743.

Janssen, P., 2004: The interaction of ocean waves and wind. *Cambridge University Press*, 300pp.

Johnson, H. K., J. Højstrup, H. J. Vested, and S. E. Larsen, 1998: On the dependence of sea surface roughness on wind waves. *J. Phys. Oceanogr.*, vol. 28, 1702-1716.

Kelly, K. A., S. Dickinson, M. J. McPhaden, and G. C. Johnson, 2001: Ocean currents evident in satellite wind data. *Geophys. Res. Lett.*, vol. 28(12), 2469-2472.

Liu, W. T., K. B. Katsaros, and J. A. Businger, 1979: Bulk parameterization of air-sea exchanges of heat and water vapor including the molecular constraints in the interface. *J. Atmos. Sci.*, vol. 36.

Liu, W.T., and Tang, W., 1996: Equivalent neutral wind. *Jet Propulsion Laboratory 96-17*, Pasadena, USA.

Maat, N., C. Kraan, and W. A. Oost, 1991: The roughness of wind waves. *Boundary Layer Meteorol.*, vol. 54, 89-103.

Milliff, R. F., 2005: Forcing global and regional ocean numerical models with ocean surface vector winds from spaceborne observing systems. *Proc. 2nd Ocean and Sea Ice SAF Workshop*, EUM P.45, ISBN 1561-1485, Perros-Guirec, France.

Milliff, R. F., and J. Morzel, 2001: The global distribution of the time-average wind stress curl from NSCAT. *J. Atmos. Sci.*, vol. 58 (2).

Monin, A. S., and A. M. Obukov, 1954: Basic regularity in turbulent mixing in the surface layer of the atmosphere. *USSR Acad. Sci. Geophys. Inst.*, No 24.

Portabella, M., and A. Stoffelen, 2007: Development of a global scatterometer validation and monitoring. *Visiting Scientist report for the EUMETSAT OSI SAF*, SAF/OSI/CDOP/KNMI/SCI/RP/141, 35pp.

Smith, S. D., R. J. Anderson, W. A. Oost, C. Kraan, N. Maat, J. DeCosmo, K. B. Katsaros, K. L. Davidson, K. Bumke, L. Hasse, and H. M. Chadwick, 1992: Sea surface wind stress and drag coefficients: the HEXOS results. *Boundary Layer Meteorol.*, vol. 60, 109-142.

Stoffelen, A., 1996: Error modeling of scatterometer, in-situ, and ECMWF model winds; a calibration refinement. *Technical report TR-193*, Koninklijk Nederlands Meteorologisch Instituut, The Netherlands.

Stoffelen, A., 1998a: Scatterometry. *PhD thesis at the University of Utrecht,* ISBN 90-393-1708-9.

Stoffelen, A., 1998b: Error modeling and calibration: towards the true surface wind speed. *J. Geophys. Res.*, vol. 103, no. C4, 7755-7766.

Stoffelen, A., 2002: Scatterometer Ocean Stress. *Proposal to the CM-SAF*, Koninklijk Nederlands Meteorologisch Instituut, The Netherlands, available at http://www.knmi.nl/scatterometer/.

Stoffelen, A., G. J. Van Oldenborgh, J. De Kloe, M. Portabella, and A. Verhoef, 2006: Development of a scatterometer ocean stress product. *Report for the EUMETSAT Climate Monitoring SAF*, 66pp.

Taylor, P. K., and M. J. Yelland, 2001: The dependence of sea surface roughness on the height and steepness of the waves. *J. Phys. Oceanogr.*, vol. 31, 572-590.

Taylor, P. K., M. J. Yelland, and E. C. Kent, 2001: On the accuracy of ocean winds and wind stress. *WCRP/SCOR Workshop on Intercomparison and Validation of Ocean-Atmosphere Flux Fields*, Bolger Center, Potomac, MD, USA.

Vialard, J., 2000: Seasonal forecast and its requirements for satellite products. *Proc. OSI SAF training workshop*, ISBN 92-9110-034-X, EUMETSAT P27, Darmstadt, Germany, 137-143.

Figure captions

Figure 1. Geographical location of both the tropical and the extra-tropical moored buoys.

Figure 2. Two-dimensional histogram of LKB estimated u_* versus ECMWF SL estimated u_* for two different extra-tropical input datasets: GTS buoys (a) and ECMWF model output (b). N is the number of data; mx and my are the mean values along the x and y axis, respectively; m(y-x) and s(y-x) are the bias and the standard deviation with respect to the diagonal, respectively; and cor_xy is the correlation value between the x- and y-axis distributions.

Figure 3. Same as Figure 2b but for the estimated z_0 parameter.

Figure 4. Normalized histogram of the stability parameter (z/L) for both the LKB model (solid) and the ECMWF SL model (dotted), using the extra-tropical ECMWF dataset as input. Negative, null, and positive z/L values correspond to unstable, neutral, and stable stratification, respectively.

Figure 5. Same as Figure 2b but with variable Charnock input to the ECMWF SL model.

Figure 6. ERS scatterometer – ECMWF (left plot) and buoy – ECMWF (right plot) wind speed bias (solid curve) and SD (error bars) as a function of the Charnock parameter (bins of 1) in the extra-tropics.

Figure 7. Difference between the LKB estimated U_n and U as a function of U, for TAO/PIRATA (tropics) (a) and GTS (extra-tropics) (b) buoy input datasets, at 4 m

height. Note that points from the right plot have been perturbed along the x-axis bins with a uniform distribution ranging [-0.5, 0.5] m/s to better discern the vertical distribution of points, i.e., the GTS speed binning (see section 2) otherwise produces a concentration of points along vertical lines.

Figure 8. Relative bias of CMOD-5 winds with respect to 10-m buoy real winds (solid) and 10-m buoy neutral winds (dotted) as a function of wind speed, for the tropical (a) and extra-tropical (b) datasets. The buoy height conversion is performed with LKB model. The dashed curve corresponds to the solid minus the dotted curve. The thick solid curve corresponds to the number of data.

Figure 9. Schematic of recommended scatterometer wind and stress conversion. The well-validated CMOD5 winds at 10m height are used as basis for geophysical conversion to friction velocity. Either real or neutral 10m winds may be transformed to friction velocity by either LKB, ECMWF or any similar SL model.

Table 1. Estimates of the wind vector SD of the true distribution and the errors of the scatterometer, LKB-derived 10 m buoy and ECMWF winds, for NWP-scale (~200 km) wind in the tropics and the extra-tropics.

Table 2. Same as Table 1, but for 50-km scale wind.

Table 3. Estimates of the wind vector SD of the true distribution and the errors of the scatterometer, LKB-derived 10 m buoy and ECMWF neutral winds, for NWP-scale (~200 km) wind in the tropics and the extra-tropics.

Table 4. Same as Table 3, but for 50-km scale wind.

Table 5. Average and SD of wind component residual biases (after wind calibration), for buoy and ECMWF winds against scatterometer winds in the tropics / extra-tropics.

Illustrations and tables

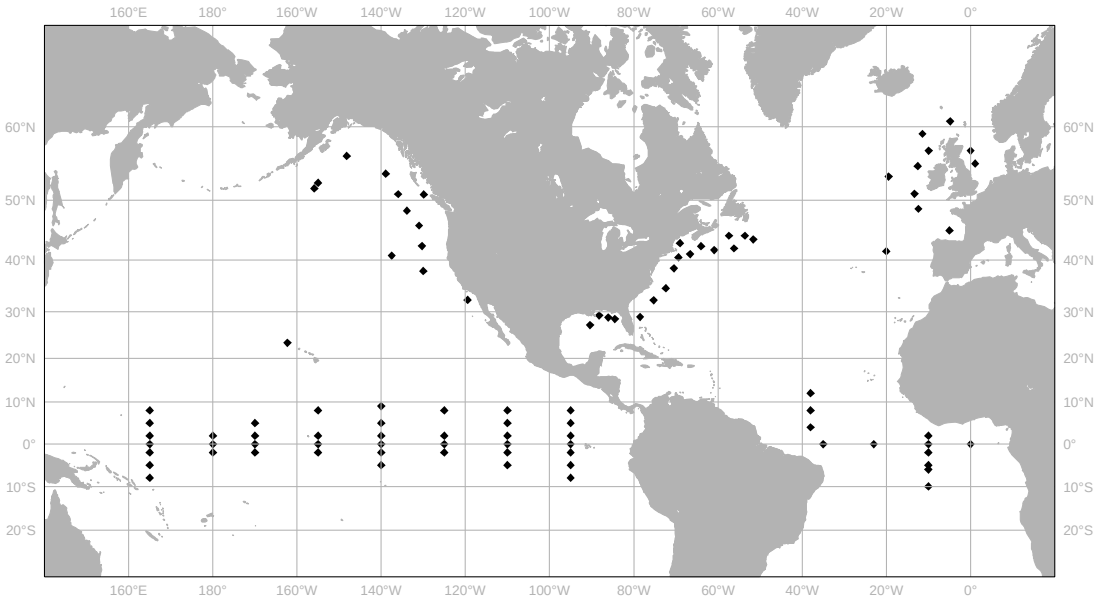

Figure 1. Geographical location of both the tropical and the extra-tropical moored buoys.

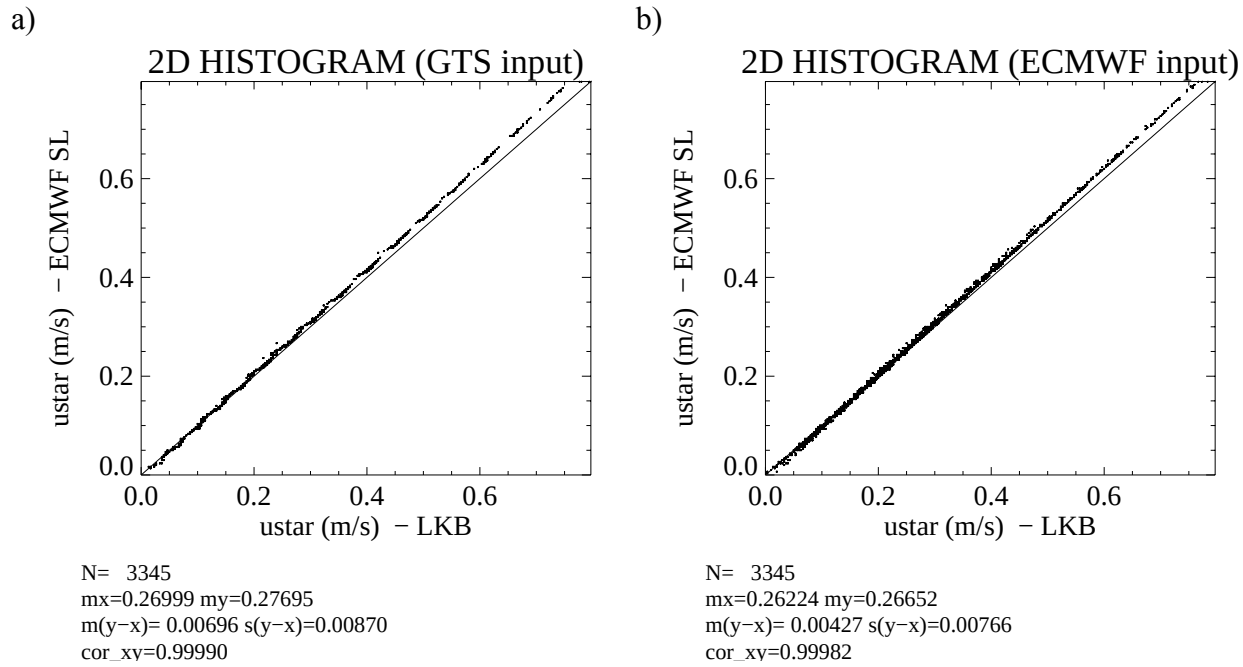

Figure 2. Two-dimensional histogram of LKB estimated u_* versus ECMWF SL estimated u_* for two different extra-tropical input datasets: GTS buoys (a) and ECMWF model output (b). N is the number of data; mx and my are the mean values along the x and y axis, respectively; m(y-x) and s(y-x) are the bias and the standard deviation with respect to the diagonal, respectively; and cor_xy is the correlation value between the x- and y-axis distributions.

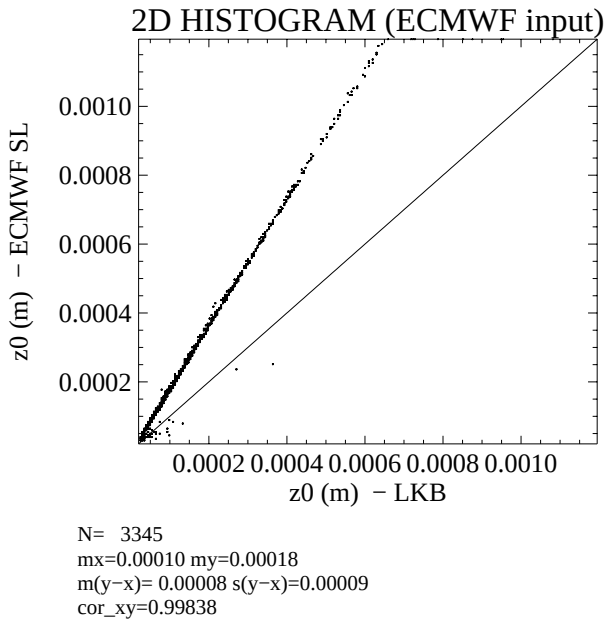

Figure 3. Same as Figure 2b but for the estimated z_0 parameter.

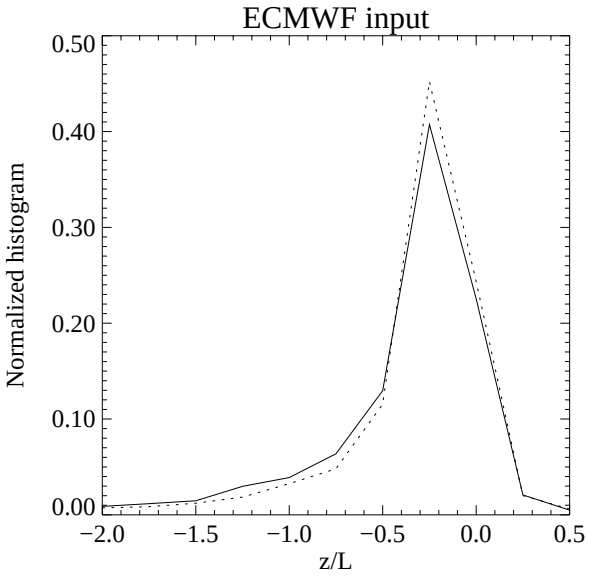

Figure 4. Normalized histogram of the stability parameter (z/L) for both the LKB model (solid) and the ECMWF SL model (dotted), using the extra-tropical ECMWF dataset as input. Negative, null, and positive z/L values correspond to unstable, neutral, and stable stratification, respectively.

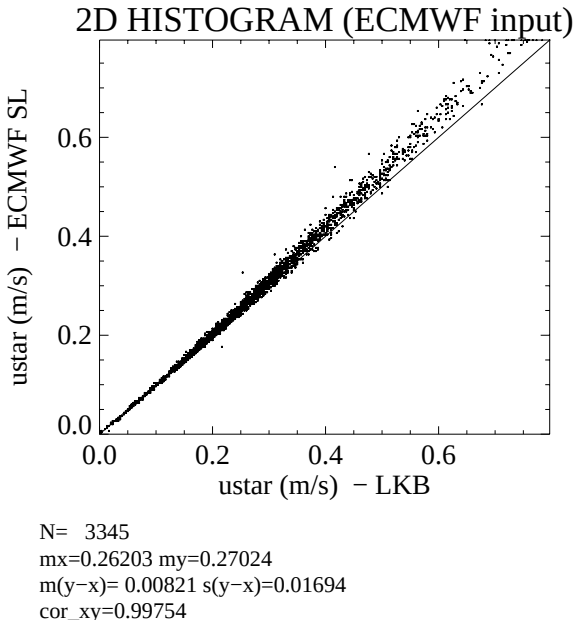

Figure 5. Same as Figure 2b but with variable Charnock input to the ECMWF SL model.

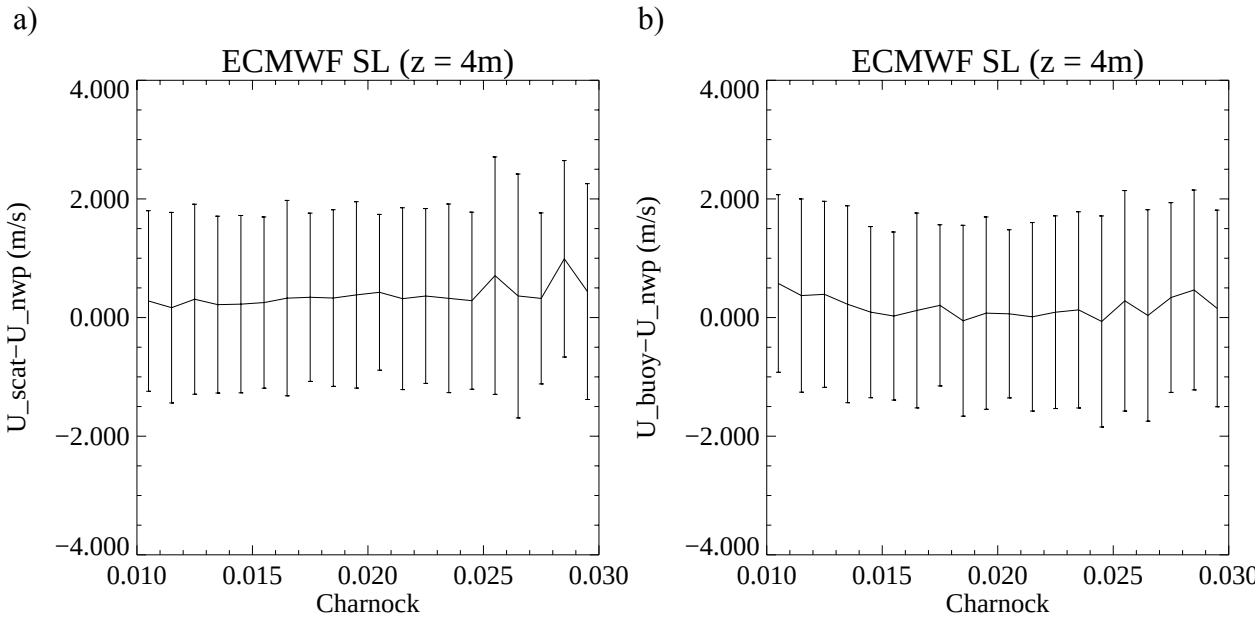

Figure 6. ERS scatterometer – ECMWF (left plot) and buoy – ECMWF (right plot) wind speed bias (solid curve) and SD (error bars) as a function of the Charnock parameter (bins of 1) in the extra-tropics.

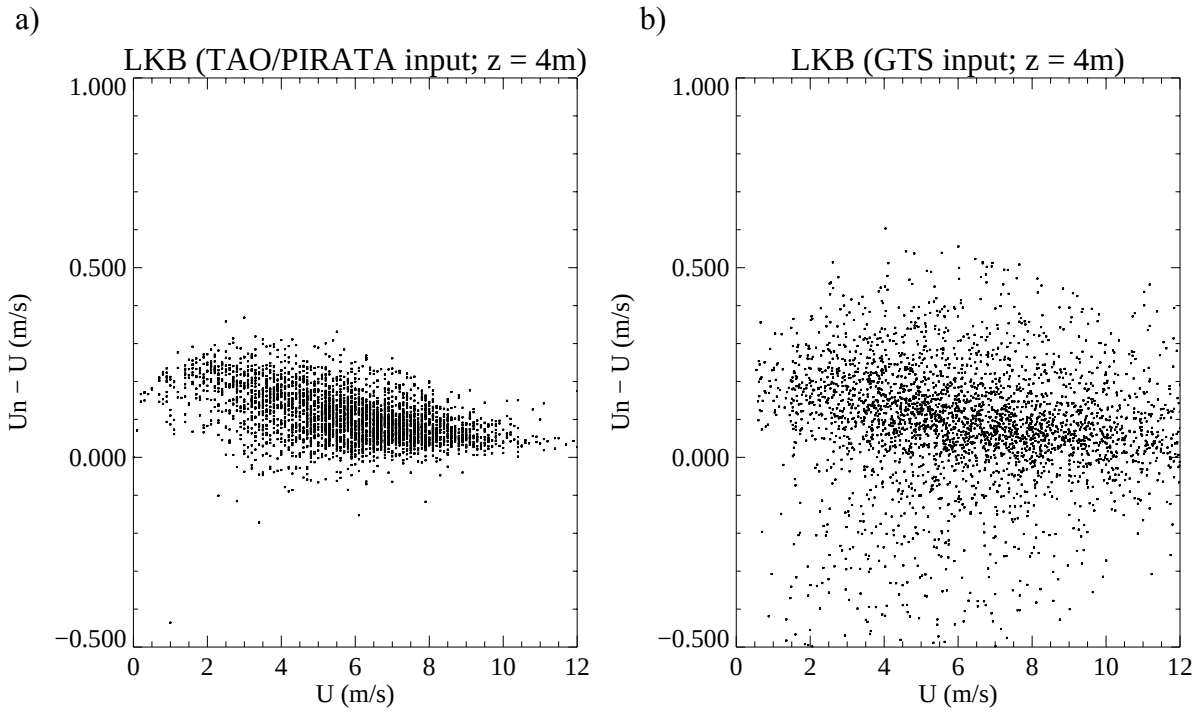

Figure 7. Difference between the LKB estimated U_n and U as a function of U, for TAO/PIRATA (tropics) (a) and GTS (extra-tropics) (b) buoy input datasets, at 4 m height. Note that points from the right plot have been perturbed along the x-axis bins with a uniform distribution ranging [-0.5, 0.5] m/s to better discern the vertical distribution of points, i.e., the GTS speed binning (see section 2) otherwise produces a concentration of points along vertical lines.

a)

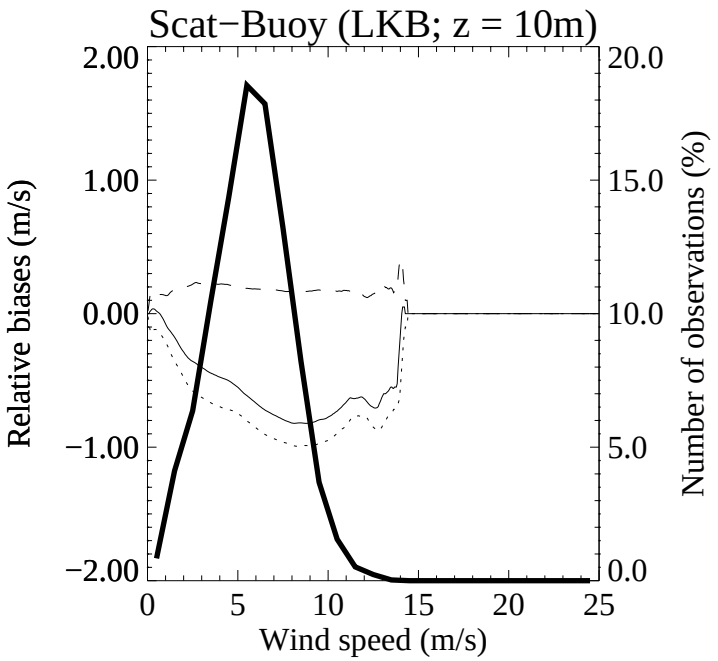

b)

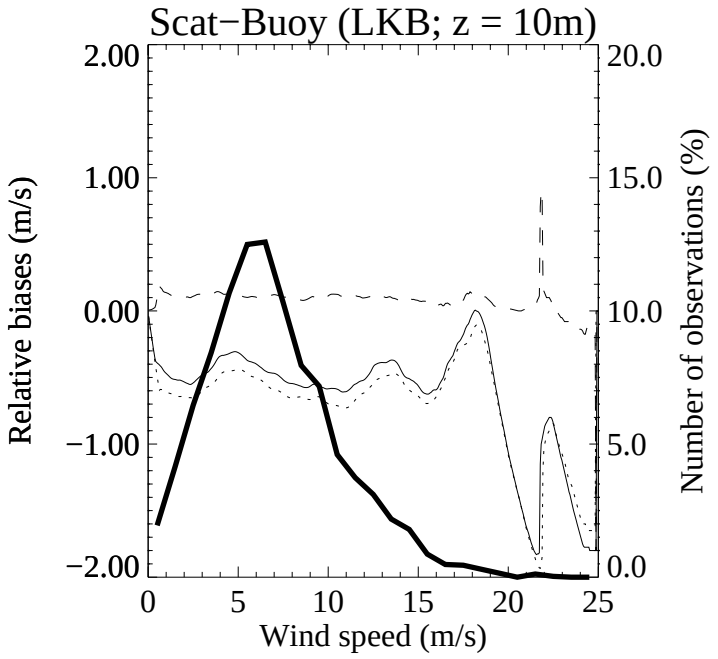

Figure 8. Relative bias of CMOD-5 winds with respect to 10-m buoy real winds (solid) and 10-m buoy neutral winds (dotted) as a function of wind speed, for the tropical (a) and extra-tropical (b) datasets. The buoy height conversion is performed with LKB model. The dashed curve corresponds to the solid minus the dotted curve. The thick solid curve corresponds to the number of data.

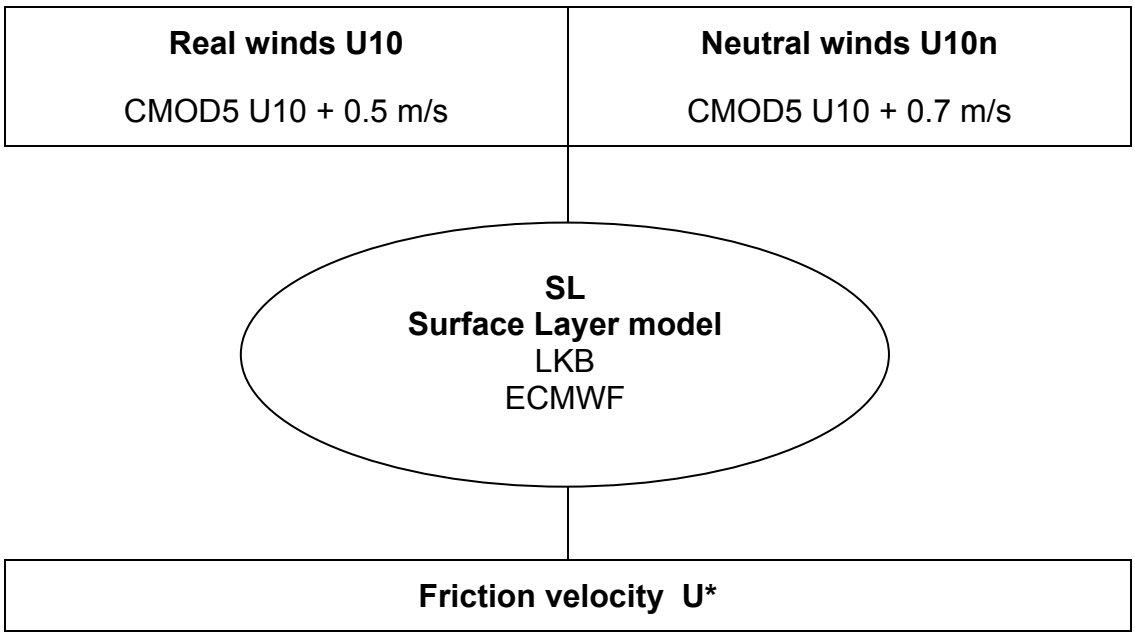

Figure 9. Schematic of recommended scatterometer wind and stress conversion. The well-validated CMOD5 winds at 10m height are used as basis for geophysical conversion to friction velocity. Either real or neutral 10m winds may be transformed to friction velocity by either LKB, ECMWF or any similar SL model.

Table 1. Estimates of the wind vector SD of the true distribution and the errors of the scatterometer, LKB-derived 10 m buoy and ECMWF winds, for NWP-scale (~200 km) wind in the tropics and the extra-tropics.

	True wind	Scatterometer	Buoy	ECMWF
Tropics (m/s)	5.79	1.36	1.63	1.91
Extra-tropics (m/s)	7.48	2.01	1.98	1.78

Table 2. Same as Table 1, but for 50-km scale wind.

	True wind	Scatterometer	Buoy	ECMWF
Tropics (m/s)	5.84	1.17	1.48	2.04
Extra-tropics (m/s)	7.58	1.60	1.55	2.16

Table 3. Estimates of the wind vector SD of the true distribution and the errors of the scatterometer, LKB-derived 10 m buoy and ECMWF neutral winds, for NWP-scale (~200 km) wind in the tropics and the extra-tropics.

	True wind	Scatterometer	Buoy	ECMWF
Tropics (m/s)	5.79	1.37	1.64	1.92
Extra-tropics (m/s)	7.49	1.97	2.01	1.78

Table 4. Same as Table 3, but for 50-km scale wind.

	True wind	Scatterometer	Buoy	ECMWF
Tropics (m/s)	5.83	1.17	1.48	2.04
Extra-tropics (m/s)	7.59	1.54	1.60	2.16

Table 5. Average and SD of the wind component residual biases (after wind calibration), for buoy and ECMWF winds against scatterometer winds in the tropics / extra-tropics.

	Buoy-Scat. U comp.	Buoy-Scat. V comp.	ECMWF-Scat. U comp.	ECMWF-Scat. V comp.
Average (m/s)	0.09 / 0.03	-0.02 / -0.12	0.21 / 0.08	-0.02 / -0.06
SD (m/s)	0.27 / 0.16	0.13 / 0.24	0.27 / 0.26	0.22 / 0.24